Ni-Al COMPOSITE COATINGS:

DIFFUSION ANALYSIS AND COATING LIFETIME ESTIMATION

[a]D.F. Susan and [b]A.R. Marder

[a]Sandia National Laboratory, Albuquerque, NM

[b]Lehigh University, Bethlehem, PA

ABSTRACT

The interdiffusion of Ni matrix/Al particle composite coatings and nickel substrates was studied using electron probe microanalysis (EPMA) and a one-dimensional diffusion model. The initial coating microstructure was a two-phase mixture of γ(Ni) and γ'(Ni$_3$Al). The coating/substrate assemblies were aged at 800 to 1100°C for times up to 2000 hours. It was found that aluminum losses to the substrate are significant at 1000°C and above. The experimental results for the diffusion of Al into the substrate were compared to model predictions based on a diffusion equation for a finite layer on an infinite substrate. Using combined experimental and model results, the effects of temperature and coating thickness were determined and a rationale was developed for coating lifetime prediction.

DISCLAIMER

DISCLAIMER

Portions of this document may be illegible in electronic image products. Images are produced from the best available original document.

1. INTRODUCTION

Nickel matrix – aluminum particle coatings can be deposited using composite electrodeposition techniques. During heat treatment, Ni-Al alloy coatings are produced with a $\gamma(Ni)$ + $\gamma'(Ni_3Al)$ microstructure exhibiting good high temperature oxidation resistance. Descriptions of coating deposition, heat treatment, and microstructure are found elsewhere [1,2]. At 800 and 1000°C, Ni-Al coatings with a $\gamma(Ni)$ + $\gamma'(Ni_3Al)$ microstructure are capable of forming protective alumina scales below an outer NiO and/or $NiAl_2O_4$ layer [2,3]. The Al concentration in the coatings is high enough and the diffusion rate is fast enough to supply Al to the surface in order to maintain alumina scale growth. However, for a thin coating on a substrate, the lifetime of the coating is not controlled directly by oxidation but by diffusion of the protective scale-forming element (Al) into the substrate [4,5]. Although the coating may be oxidation resistant initially, if the Al content drops below a critical level, it may not be possible to form a continuous surface alumina layer at long times. When the Al level is very low, as previous studies on dilute Ni-Al alloys have shown [6-9], significant internal oxidation attack may occur.

Electron probe microanalysis (EPMA) results, described in this paper, showed significant Al losses from Ni-Al coatings into a Ni substrate with prolonged isothermal exposure at 1000°C. Although the coatings generally form protective scales, the long-term results at 1000°C indicate a significant mass increase due to oxidation [2]. In addition to defect-related oxidation, such as interfacial oxidation due to coating delamination, increased attack in some areas may be caused by local decreases in Al content. To avoid internal oxidation or growth of nonprotective scales (e.g. NiO), it is important to study the diffusion of Al from the coating into the substrate. This paper discusses experimental measurements and mathematical modeling of Al diffusion from Ni-

2

Al coatings into a Ni substrate, including the effects of varying temperature and coating thickness. Using a combination of observed Al diffusion and model results, a rationale for estimating coating lifetime is also developed.

2. EXPERIMENTAL PROCEDURE

2.1. High Temperature Exposure of Ni-Al Composite Coatings

Nickel matrix – aluminum particle composite coatings were deposited on all sides of Ni200 alloy substrates (substrate dimensions approx. 12 x 12 x 2 mm). The as-deposited coatings contained about 20 volume percent Al particles. The coating deposition procedure is found elsewhere [1,2]. The coated samples were then vacuum heat treated at 825°C for three hours to produce a γ(Ni) + γ'(Ni$_3$Al) coating microstructure. Prior to long-term diffusion experiments, the six coating surfaces were prepared to an 800 grit finish. Coating thickness was about 100-125 μm after final sample preparation. The samples were then ultrasonically cleaned in alcohol, rinsed, and dried. Long-term exposure tests were conducted in tube furnaces at 800 and 1000°C, which are above and below, respectively, the maximum service temperature for Ni$_3$Al materials (about 900°C) [10]. Dry air was passed through drierite (CaSO$_4$) prior to entering the furnace at a flow rate of 50 ml/min. The dry air atmosphere was chosen (instead of vacuum) to study the simultaneous oxidation behavior of the coatings [2]. Individual samples were removed from the furnace after 10, 50, 100, 200, 500, 1000, and 2000 hours and cooled to room temperature. Additional diffusion experiments were conducted at 1100°C for up to 300 hours as accelerated tests to obtain Al diffusion profiles.

2.2. Scanning Electron Microscopy and Electron Probe Microanalysis

Following high temperature aging, the coating/substrate assemblies were cross-sectioned, mounted in epoxy, and prepared using standard metallographic techniques. Characterization was performed with a JEOL 6300F field emission scanning electron microscope (SEM) operated at 15kV accelerating voltage. The SEM was operated in both secondary and backscatter (BSE) modes. In general, the epoxy mounted samples were carbon coated prior to analysis to avoid charging effects.

Electron probe microanalysis (EPMA) was performed on a JEOL 733 SuperProbe equipped with wavelength dispersive spectrometry (WDS) to quantitatively identify the composition of phases in the coating/substrate diffusion couples. The mounted and polished samples were surrounded with carbon tape to avoid charging during analysis (carbon coating was not used during EPMA analysis). Pure element standards were used for analysis of aluminum and nickel. A pure Al_2O_3 standard was employed for oxygen analysis. For metallic element analyses, the accelerating voltage was 20 kV and the probe current was 14 nA. For oxygen analysis, a probe current of 35 nA was needed to increase the oxygen x-ray counts. A computerized $\phi\rho z$ correction scheme was implemented that is particularly suited for analyzing light elements with high absorption corrections. Probe traces were conducted from the coating into the substrate with a step size of two microns within large single-phase regions to document the phase compositions. Larger step sizes were used between these regions to decrease the total analysis time within the coating. As the coating/substrate diffusion zone was approached, the step size was again reduced, depending on sample diffusion temperature and time. Within the diffusion zone, the step size was 2 to 5 μm, depending on diffusion temperature and time. For example, in the 1000°C/1000hr. sample the step size was 5 μm because of the large size of the

4

diffusion zone. Backscattered electron photomicroscopy was also performed to characterize phase layer depletion within the coatings and to document the microstructure in the probe trace regions.

3. EXPERIMENTAL RESULTS

3.1. *Coating morphology and γ' depletion*

After electrodeposition and heat treatment, the Ni-Al composite coatings consist of a two-phase mixture of γ(Ni) + γ'(Ni$_3$Al) with blocky morphology [2,3]. Small pores are also found within the coatings. When samples are exposed to high temperature for long times, depletion of the γ' phase occurs near the coating surface (just below the external oxide layer). In addition, γ' depletion also occurs near the coating/substrate interface. The widths of both depletion zones increase with time, diminishing the γ + γ' layer within the coating. Figure 1 shows BSE photomicrographs of a Ni-Al coating after initial heat-treatment and subsequent exposure for 50 hours at 1000°C. Slight contrast is found between the γ and γ' phases, with γ' appearing darker. The coating was initially fully γ + γ', but after 50 hours at 1000°C, a γ' depletion zone has developed about 65 μm wide near the coating/substrate interface. A γ' depletion layer about 15 μm deep is found near the coating surface. Due to these γ' depletion layers, the two-phase γ + γ' layer of the coating has decreased to about 50 μm in width. The width of the two-phase layer continues to decrease with time (from both directions) and, eventually, the entire coating becomes single phase γ. At 1000°C, the two-phase layer is fully depleted between 100 and 500 hours of exposure. To accelerate diffusion and test a diffusion model (see Section 4 below), samples were also exposed at 1100°C. At 1100°C, γ' depletion

5

occurred in less than 50 hours. In contrast, at 800°C, the Al diffusion rate is slower and a significant two-phase $\gamma + \gamma'$ region remains even after 2000 hours as shown in Figure 2. In the 800°C sample, a γ' depletion zone only about 30 μm wide is found near the coating/substrate interface. Very little γ' depletion is found near the coating surface, but there may be a slight decrease in the size and volume fraction of γ'. Figure 3 summarizes the depletion of the two-phase $\gamma + \gamma'$ layer as a function of time for 800, 1000, and 1100°C. The results show that the 1000 and 1100°C coatings become single phase at relatively short times. Therefore, for long-term diffusion at 1000 and 1100°C, it is possible to model these coatings as single-phase layers. (It was not possible to determine exact depletion kinetics in Figure 3 because samples were not exposed at very short times. Note also that the initial $\gamma + \gamma'$ layer thickness is plotted at 0.01 hours.)

3.2. Electron probe microanalysis results

Electron probe microanalysis (EPMA) was used to measure Al interdiffusion between the coating and substrate at 800 to 1100°C. Figure 4a exhibits a typical 800°C EPMA trace through the coating perpendicular to the coating/substrate interface, across the diffusion zone, and into the substrate. Several data points were analyzed in each phase and the Al compositions correspond well with the Ni-Al phase diagram (Figure 5) at 800°C. At the coating/substrate interface, diffusion occurs in the γ phase and the Al concentration decreases and Ni concentration increases until the substrate composition (commercially pure nickel) is reached. Figure 4b shows an expanded view of the Al composition profiles after aging at 800°C for 100 and 1350 hours. The γ and γ' compositions are labeled in the figure. Many data points correspond to interphase

6

interfaces and the measured composition lies between the γ and γ' values. Figure 6a shows a typical EPMA trace (100 hours) at 1000°C. A thin region of two-phase $\gamma + \gamma'$ remains within the coating after 100 hours at 1000°C. A summary of the Al composition profiles from 1000°C samples is shown in Figure 6b for times up to 2000 hours. In addition, to further characterize the Al depletion behavior, coatings were diffused at 1100°C. These experiments were performed to accelerate diffusion and test a diffusion model (This temperature is too high to be considered for practical coating applications.) Figure 7a displays an Al composition profile for 10 hours at 1100°C. A thin two-phase $\gamma + \gamma'$ region remains after 10 hours at 1100°C. Figure 7b summarizes diffusion results for up to 312 hours at 1100°C. For the long-term experiments, only the composition near the coating surface was measured to document the Al surface content for comparison to a diffusion equation.

With increasing time, the width of the coating/substrate diffusion zone generally increases. However, at 800°C (Figure 4), the γ phase composition remains at its Al saturation value in the majority of the coating for at least 2000 hours. At 1000°C and above, an important feature of the diffusion profiles is that the γ phase composition drops below its Al solubility limit at longer times. This behavior marks the onset of full depletion of the two-phase $\gamma + \gamma'$ region, i.e. after depletion of γ', the γ phase Al composition begins to decrease.

The probe traces generally display a smooth Al concentration profile. However, for long times at 1000°C (Figure 6b), a region was found where Al content is relatively constant. This behavior occurs near an oxide and/or nitride zone [2], which is a result of oxygen diffusion along the coating/substrate interface. In classic diffusion analyses, experiments are usually performed in a vacuum or inert atmosphere and such phase formation would not be encountered. As shown

7

below, in samples where these coating/substrate interface effects did not occur, the diffusion results in the present study (dry air atmosphere) are similar to results found in previous Ni-Al diffusion studies performed under vacuum conditions.

3.3. Interdiffusion coefficients in γ phase at 800 and 1000°C

To study the diffusion of Al into a Ni substrate, the interdiffusion coefficient must be known in the Ni-Al system. The Boltzmann-Matano method can be used to determine the interdiffusion coefficient, D, as a function of Al content at a given temperature [11,12]. The Boltzmann-Matano method is a graphical technique to extract the interdiffusion coefficient from the Al concentration profile obtained by EPMA. An EPMA profile of a binary Ni-Al coating on a Ni substrate, for example Figure 8 (50 hrs. at 1000°C), can be used to determine D with this method.

Several researchers, including Watanabe et al. [13] and Jansenn et al. [14], have studied diffusion in the Ni-Al system. Watanabe et al. used a modified Matano-Boltzmann method (which considered changes in molar volume due to Al diffusion into Ni) to determine D in the γ phase from 900 to 1200°C. The unmodified Matano technique [11,12] was used in the present research to determine D-values at 800 and 1000°C. The interdiffusion coefficients were then used in modeling coating lifetime (Section 4) based on aluminum diffusion from the coating into the substrate. Figure 9 displays D (in cm^2/sec) as a function of Al content obtained from the coating/substrate diffusion couple results in the present study. The interdiffusion coefficients are similar to those found by Watanabe et al. at 1000°C. Slight differences between the present results and those of Watanabe et al. may have been caused by microstructural factors or the presence of oxygen (dry air in this study vs. vacuum in Watanabe et al. [13]). In addition,

8

Watanabe et al. used a modified Matano method [15], in which the molar volume changes (as Al diffuses into Ni) are considered. The simple Matano technique used in this study appears adequate for the present purposes. The D-values at 800°C are reasonable when compared to the previous work at higher temperatures. The Arrhenius relationship describes the effect of temperature on the interdiffusion coefficient, and can be used to determine the activation energy for diffusion. When the 800°C values from the present study are combined with Watanabe's data from higher temperatures, an average activation energy, Q, of 258 ± 8 kJ/mol was obtained for the γ phase. This agrees well with the activation energies in the γ phase obtained by other researchers [13]. These results highlight the ability of the composite plating technique to produce diffusion couples where one end member is an alloy produced during initial high temperature exposure of the composite coating.

For the diffusion analysis presented below, average D-values obtained from the EPMA data of the present work were used for 800 and 1000°C. This was determined to be acceptable since Figure 9 shows only a slight dependence of D on Al concentration. For prediction of diffusion behavior at 900 and 1100°C, the average D-values from Watanabe et al. [13] were used. In addition, the interdiffusion coefficient for 700°C was extrapolated as 1.5×10^{-14} cm^2/sec. A summary of the interdiffusion coefficients for use in modeling coating/substrate interdiffusion is given in Table I.

Table I. Average γ phase interdiffusion coefficients.

Temperature (°C)	Avg. Interdiffusion Coefficient, D, (cm^2/sec)
700	* 1.5×10^{-14}
800	2.0×10^{-13}
900	3.0×10^{-12}
1000	1.2×10^{-11}
1100	1.5×10^{-10}

* extrapolated

4. DIFFUSION MODEL

4.1. Model description

The Al composition generally displays a smooth decrease through the γ phase diffusion zone between the coating and the substrate. At high temperature, the γ phase Al content decreases below the Al solubility limit after full γ' depletion has occurred (Figures 6, 7). A solution to Fick's second law was employed to predict the Al compositional change as a function of diffusion time at a given temperature [11,16]. The interdiffusion coefficients for 800 to 1100°C, determined by the Boltzmann-Matano method and listed in Table I, were used in the equation.

The geometrical construction for modeling diffusion comprised a coating of finite thickness, h, on a semi-infinite substrate. A schematic diagram of this geometry is shown in Figure 10. The initial distribution is as follows:

$$C = C_o \text{ for } 0 < x < h \text{ and}$$

$$C = 0 \text{ for } x > h \quad \text{at } t = 0.$$

10

It is assumed that, during the time of the experiment, the concentration changes do not reach the outer boundary of the substrate, i.e. the substrate is semi-infinite. The resulting composition distribution is:

$$C = (C_o / 2)\left[erf\left(\frac{h+x}{2\sqrt{Dt}}\right) + erf\left(\frac{h-x}{2\sqrt{Dt}}\right)\right]$$ (1)

where C = concentration, C_o = initial coating composition, erf = the error function, h = coating thickness, x = distance, D = interdiffusion coefficient, and t = diffusion time [11,16]. The x = 0 coordinate corresponds to the coating surface. The distribution is symmetric about x = 0 so the system may be cut in two by a plane at x = 0 without affecting the concentration distribution [11,16] and, therefore, only one half of the model distribution is shown in Figure 10. A discussion of Equation (1) is given by Jost in Ref. [11].

4.2. Model discussion and assumptions

4.2.1. Homogeneous System

The solution to Fick's second law described above applies to a single-phase system with two different end member compositions at time t = 0. In the present study, the coatings begin as two-phase alloys with γ + γ' microstructure. However, depletion of the γ' phase occurs relatively quickly, especially at 1000 and 1100°C (Section 3 above). In Figure 3, it was shown that γ' is fully depleted in less than 50 hours at 1100°C, which is a small fraction of the total diffusion time. Therefore, Equation (1) is strictly valid for times after about 10-50 hours at 1100°C. At 1000°C, complete γ' dissolution occurs between 100 and 500 hours so Equation (1) is strictly

11

valid after a few hundred hours at 1000°C. In the following analysis, the model was applied after 25 hours and 150 hours for 1100 and 1000C, respectively.

The initial coating composition is taken as the solubility limit of Al in γ, which was determined from the EPMA results presented above. In Figures 4 to 7, the γ solubility limit is a constant value in the diffusion profiles. The γ phase Al concentration remains close to this limit during the early stages of diffusion. Only after the γ' phase is fully depleted, e.g. between 100 and 500 hours at 1000°C, the γ composition begins to drop below its solubility limit. At this time, the diffusion process "sees" the finite thickness of the coating. The equation is strictly applicable after this point is reached. At longer times, the γ phase composition smoothly decreases within the coating (Figures 6 and 7). The application of the model at lower temperatures is somewhat more difficult. At 800°C, the $\gamma + \gamma'$ phase layer remains within the coating for long times and the model is not strictly valid. However, Equation (1) can still be used to estimate the kinetics of Al diffusion and a discussion of the 800°C results is presented later. The effects of other microstructural features, such as grain size and pores, are also not considered in the diffusion model.

4.2.2. Oxidation and Composition Effects

Other assumptions are implicit in the model presented above. First, the effects of oxidation reactions at the surface are not considered. As mentioned previously, diffusion experiments are usually performed in vacuum. However, if a thin, protective Al_2O_3 scale forms on the coating surface, it effectively isolates the coating from the atmosphere, as shown in previous studies [4,5]. Previous research has shown that, for an Al_2O_3 former, coating lifetime is

12

limited by diffusion and not by oxidation reactions directly (until the Al content drops below a critical level). Therefore, the analysis only holds for coatings that form protective Al_2O_3 scales. Also, the interdiffusion coefficient is assumed constant within the γ phase (not a function of composition). As shown in Section 3, the D-value increases only slightly with Al content so this assumption appears valid.

Another important factor in this study is that, although γ' depletion occurs near the surface, accelerated oxide-related Al depletion does not occur below the surface oxide. For a given diffusion time, the Al composition is relatively constant through the coating (Figures 4 - 7). As diffusion continues, the entire coating Al content decreases as Al is lost to the substrate. No accelerated decrease in γ phase Al content is found adjacent to the oxide, at least within the resolution limit of EPMA. Constant Al compositions across a sample were also found by Nesbitt et al. [17] during high temperature oxidation of NiAl and by Nesbitt and Heckel [18] during oxidation of Ni-Cr-Al alloys. This behavior is different from that observed in some other alloys. For example, Strutt and Vecchio [19] oxidized thin sheets of a Cr_2O_3-forming alloy (347 stainless steel) at 650-815°C. A sloping Cr concentration profile was found below the oxide surface. To illustrate the two types of behavior, a schematic diagram is shown in Figure 11. In the Cr_2O_3-forming alloy, a sloping Cr profile is found adjacent to the oxide. In the Al_2O_3-forming alloy, a flat Al concentration profile is found below the oxide surface. In general, the diffusion of Cr is slower than diffusion of Al at a given temperature. In addition, Cr_2O_3 growth kinetics are faster than Al_2O_3 growth kinetics [20]. Therefore, the formation and growth of Cr_2O_3 (at 650-815°C) produces a Cr-depleted region directly below the oxide layer. To analyze simultaneous oxidation and diffusion, Strutt and Vecchio [19] used an equation that also

13

accounts for the oxidation reaction (through use of a parabolic rate constant for oxidation)[19,21]:

$$C = C_o - \sqrt{\frac{\pi K_p}{2D}}\left[erfc\left(\frac{2h}{2\sqrt{Dt}}\right) + erfc\left(\frac{4h}{2\sqrt{Dt}}\right)\right]. \qquad (2)$$

In this equation, K_p = the parabolic oxidation rate constant, h = foil thickness, erfc = error function compliment, and the other parameters are the same as in Equation (1). To use this equation, the parabolic rate constant must be known under the given conditions. The K_p term in Equation (2) accounts for the depletion of the scale forming element (Cr) adjacent to the oxide. Although Equation (2) could also be used to study Al_2O_3 formers, the coatings in the present study did not generally follow parabolic oxidation kinetics [2], so an estimate of K_p would have been necessary. For the Al_2O_3-forming coatings of the present study, the simpler Equation (1) was used, which considers only coating/substrate interdiffusion. In the present study, aluminum diffusion is fast enough to maintain an Al_2O_3 scale without Al depletion at the oxide/coating interface. If secondary Al depletion were to occur below the oxide surface, Equation (1) may not be valid.

4.2.3. Coating Thickness and Kirkendall Effects

It is assumed that the coating thickness, h, remains constant throughout the diffusion experiment. If a thin, protective Al_2O_3 scale forms on the coating surface, it does not significantly decrease the coating thickness. If, however, Al_2O_3 is unable to form and accelerated oxidation attack occurs, the model will break down. In addition, the Kirkendall

14

effect is not considered. Due to differences in the diffusion rates of Al and Ni, the Kirkendall effect occurs in the Ni-Al system [22,23]. The Kirkendall effect will cause a shift in the coating/substrate interface during diffusion, thereby slightly changing the coating thickness. In the present study, it was assumed that Kirkendall effects would not cause major changes in coating thickness. In general, the initial coating thickness, h, is an important parameter controlling the diffusion process. Thicker coatings provide a larger reservoir of Al and will have longer lifetimes. The effect of varying the initial coating thickness will be discussed below.

4.3. Comparison of model and experimental results

4.3.1. Diffusion Profiles

A typical calculated diffusion profile (50 hr., 1000°C) from Equation (1) along with experimental (EPMA) results was displayed above in Figure 8. The experimental results agree relatively well with the calculated curve. The initial coating composition, C_o, was taken as 0.155 atom fraction Al and the coating thickness, h, was 100 μm. An interdiffusion coefficient of $D = 1.2 \times 10^{-11}$ cm^2/sec was employed. The results indicate that Equation (1) is able to adequately predict the interdiffusion behavior of a Ni-Al coating on a Ni substrate. Similar agreement was found for other diffusion temperatures and times (except for very long times at 1000°C due to interfacial oxide/nitride formation, as discussed previously).

4.3.2. Surface Al Concentration

Figure 8 demonstrated the use of Equation (1) for analyzing composition as a function of distance, x, for a given diffusion time and temperature. By holding x constant, the equation can also be used to monitor the change in Al content at a particular position as a function of time.

15

For high temperature oxidation of Ni-Al coatings, the coating surface, x = 0, is of prime importance. A sufficient Al content is needed at the surface to maintain the growth of an Al_2O_3 scale. Figure 12 shows the results for the change in Al concentration at the coating surface (x=0) as a function of time at 800, 1000, and 1100°C. For each temperature, the model was applied after the approximate time of depletion of the γ' phase, i.e. when the coatings became single phase γ. Each EPMA data point in Figure 12 is an average of the first few data points below the oxide (leftmost data points in Figures 4 to 7). At early aging times, these values correspond to approximately the γ phase solubility limit for Al at each temperature. A summary of the parameters used in the model is given in Table II. Based on Figure 12, the experimental results show good agreement with the calculated values. Some deviation occurs at long times at 1000°C, most likely due to interfacial oxide/nitride formation [2]. It should be noted also that coating porosity may produce error between measured and calculated Al concentrations. Porosity will effectively decrease the amount of Al available for diffusion with a given coating thickness (alternatively, porosity can be considered to effectively reduce the initial coating thickness).

At 1000°C, the surface Al content begins to decrease after about 200 hours. The surface Al content falls off quickly at 1100°C. Note that the actual average coating composition at early times (before the model is applied) is between the γ and γ' compositions and is, therefore, slightly higher than the γ phase C_o compositions in Figure 12.

16

Table II. Parameters used to calculate surface Al content as a function of time.

Temperature (°C)	Interdiffusion Coefficient, D, (cm^2/sec)	C$_o$ (atom fraction Al)	h (µm)
700	1.0×10^{-14}	0.10	100
800	2.0×10^{-13}	0.115	100
900	3.0×10^{-12}	0.13	100
1000	1.2×10^{-11}	0.155	100
1100	1.5×10^{-10}	0.16	100

4.3.3. Model Results at 800°C

As discussed above, Equation (1) applies to the γ phase only. At high temperatures, γ'

depletion occurs relatively quickly but, at 800°C, the γ' phase is still present after long times.

Therefore, the γ' EPMA compositions measured at early times are not plotted in Figure 12. The

equation was nevertheless used to estimate the 800°C coating behavior, understanding the

limitation of using a one-phase model for the two-phase coatings at low temperature. In this

system, the γ and γ' compositions are similar (Figure 5). In other systems with two-phase layers,

in which the two phases have widely differing composition, larger error would be involved with

the application of Equation (1). The model was applied after 2000 hours which was the longest

experimental time used. This procedure was believed to give a conservative estimate for the

long-term depletion of Al since the γ' regions, which are still present at 2000 hours, would add to

the Al reservoir within the coating. Based on Figure 12, at 800°C the coating composition

remains constant for long times (about 10,000 hours) and then gradually decreases. Since no

decrease in the surface Al content was found within the experimental times, a direct comparison

cannot be made between the long-term model results and experimental EPMA values.

However, the data can be viewed as a lower bound, i.e. for the starting Al coating composition

and thickness, the Al surface concentration is constant for at least 2000 hours. To fully compare experimental and model results at 800°C, very long-term tests would be needed, which was not feasible in this study. With a similar procedure, the model was used to predict the surface Al content during coating/substrate interdiffusion at other temperatures not tested experimentally. Figure 13 shows the predicted curves for 900 and 700°C along with the calculated results for 800, 1000, and 1100°C from Figure 12. These results, along with knowledge of oxidation behavior as a function of surface Al content, can be used to estimate coating lifetime as described below.

4.3.4. Surface Al Depletion and Coating Thickness Effect

Based on Figures 12 and 13, the time for the surface Al content to significantly decrease can be estimated. Figure 14 is a plot of the time to "onset of surface depletion" (time to 1% decrease in Al) vs. temperature. As the temperature is increased, the onset of depletion occurs much more quickly. The results are important for design purposes for coated components exposed to high temperature. The 700-800°C range appears to be a practical use range for Ni-Al composite coatings. At higher temperatures, Al depletion occurs more quickly and, therefore, a decrease in oxidation resistance is expected.

The effect of coating thickness on the predicted surface Al concentration is shown in Figures 15 for 1000°C. Based on Equation (1), as coating thickness is increased, the Al concentration is higher at any given time. Therefore, the time to the onset of depletion is also increased. For example, if coating thickness is doubled from 75 to 150 μm, the depletion onset time increases from about 100 hours to about 500 hours at 1000°C. If coating thickness is

18

increased to 300 μm, the time to onset increases to about 2000 hours. The results in Figure 15 show the importance of coating thickness as a design parameter.

5. COATING LIFETIME ESTIMATION

In the following section, the Al diffusion results described above will be discussed with reference to the oxidation results from previous work [2,24]. In another part of this study, the effect of Al content on the oxidation behavior of Ni-Al alloys was determined at 800 and 1000°C. It is known that increasing Al content and/or temperature promotes Al_2O_3 scale formation [2,10,24]. At 800°C, a dilute γ alloy showed internal oxidation and inability to form a continuous Al_2O_3 layer. (The results were based on 50-hour TG experiments. A continuous layer may be formed at the base of the internal oxide zone at longer times.) At this temperature, a critical Al content of about 6.5 to 7 wt. % (about 12-13 at. % Al) is needed to form a continuous Al_2O_3 layer. The analysis presented in Section 4 shows, however, that the Al composition of a Ni-Al coating on a Ni substrate changes with time. This dynamic situation means a coating that is initially an Al_2O_3-former may not be able to maintain an Al_2O_3 layer at long times during oxidation. The γ phase composition at 800°C is only about 11.5 at. % Al as shown in Figure 12. However, the actual coating composition is about 17 at. % -- between the γ and γ' compositions. When γ' is fully depleted, Al content in the γ phase will begin to drop and the coating may not be able to form an Al_2O_3 scale. Therefore, the time to onset of depletion (Figures 12-14) can be used as an estimate of coating lifetime at 800°C. At 1000°C, the γ alloy (6.2 wt. % Al) was able to form a healing Al_2O_3 layer after about 7 hours of oxidation [2]. Higher Al alloys (including Ni-Al composite coatings) were able to form protective Al_2O_3 layers below an outer $NiAl_2O_4$ scale. In Figure 16, the measured and calculated plots of surface Al content vs. time are shown

19

for 700 to 1100°C. The surface Al composition of 12 at. %, the approximate composition at which bulk alloys begin to lose Al_2O_3 scale-forming ability, is superimposed as vertical lines for 900 to 1100°C. For 700 ad 800°C, the onset of depletion is used as a lifetime estimate. The time to reach this Al content can be used as a rough estimate of coating lifetime. This type of analysis suggests that coatings may last about 2000 hours at 900°C, 8000 hours at 800°C, and 80,000 hours at 700°C.

5.1. Composition and microstructural effects on coating lifetime

It must be emphasized that the coating lifetimes shown in Figure 16 are estimates only. The exact oxidation conditions, substrate composition, and coating microstructure will affect coating lifetime. For example, the oxidation results in this study were obtained for dry oxidation. If moisture or other corrosive species are present in the atmosphere, the coating lifetime may be reduced. Substrate composition also has a large effect on coating lifetime [5,25]. For a pure Ni substrate, there is a large driving force for Al diffusion and the substrate acts as a very effective Al sink. Levine [5] and Fink and Heckel [25] have shown that substrates with higher Al content are less effective Al sinks and, therefore, less Al diffuses from the coating into the substrate. Therefore, if the substrate Al composition is increased, coating lifetime would be expected to increase.

Microstructural factors are also not considered in the coating lifetime estimates. The small grain size of Ni-Al composite coatings may increase coating lifetime (compared to large-grain material) at lower temperatures [26,27]. Perez et al. found that small grain size may enhance Al diffusion to the surface to form a protective Al_2O_3 layer. At higher temperatures, grain size is expected to have less effect because bulk diffusion rate becomes comparable[26,27].

20

Finally, it should also be noted that *after an Al$_2$O$_3$ scale is formed,* the Al content of the alloy may drop to very low levels without loss of protection. For example, a bulk 6 wt. % alloy at 1000°C forms a NiO layer, an internal oxide zone, and finally a healing Al$_2$O$_3$ layer at the base of the internal oxidation zone [2]. Once the healing layer is formed, it provides adequate protection to the alloy. Long-term oxidation results for Ni-Al coatings [2] show that an Al$_2$O$_3$ scale is present after 1000-2000 hours when the Al content has dropped to low levels (about 5 at. % Al). Thermodynamically, an Al$_2$O$_3$ scale is stable at very low Al concentrations [28]. Nevertheless, caution should be used when assigning coating lifetimes. The estimates shown in Figure 16 should be conservative since the lifetimes are based on short-term oxidation results of low Al alloys. An alloy of similar Al content, *for which an Al$_2$O$_3$ scale was already pre-formed,* may remain protected for longer times.

5.2. Thermal cycle effects

The experimental and calculated diffusion results in this study are for isothermal tests only. Thermal cycling may cause Al$_2$O$_3$ scale spallation, as studied by many researchers (e.g. Refs. [29,30]). During cooling of Ni-Al composite coatings from 1000°C to room temperature, oxide scale spallation was observed [2]. If spallation occurs after significant Al depletion has taken place below the surface, an Al$_2$O$_3$ scale may not be able to reform. The effects of thermal cycling on oxidation lifetime have been studied by Nesbitt et al. [18,25,31-33]. In general, oxidation lifetime is reduced if spallation occurs, due to accelerated loss of Al. In the present study, thermal cycling and spallation effects were not considered. In future work, combined thermal cycle oxidation tests and EPMA analysis below the surface may be used to monitor Al losses and predict component lifetime during thermal cyclic exposure.

21

6. CONCLUSIONS

The interdiffusion between a Ni-Al composite coating and Ni substrate has been studied experimentally using EPMA and modeled with a 1-D Fick's second law diffusion equation. The following conclusions can be drawn from this work:

1. The diffusion of Al from Ni-Al composite coatings into a Ni substrate occurs with interdiffusion coefficients similar to previous studies at 800 and 1000°C. The results show that the composite electrodeposition process may be used as a means to produce diffusion couples for long-term diffusion studies.

2. EPMA analysis in this study showed significant γ' depletion within the coatings and Al diffusion to the Ni substrate at 1000 and 1100°C. At 800°C, little or no γ' depletion is found and Al loss to the substrate is modest after 2000 hours. Coating/substrate interdiffusion can be modeled by a simple solution to Fick's second law and good agreement is found between EPMA data and calculated values for Al composition at the coating surface. In addition, the equation can be used to quantitatively show the beneficial effect of increasing coating thickness to maintain a higher surface Al content for longer times.

3. Based on the Al depletion characteristics and known oxidation behavior for various Ni-Al alloys, coating lifetime can be estimated. By monitoring the surface Al concentration, the time is found at which the surface Al content falls below the critical level needed for Al_2O_3 formation. The EPMA and analytical results show that coating lifetimes at 700-800°C are long enough for

practical coating applications. At 1000 and 1100°C, significant Al depletion occurs after a few thousand or several hundred hours, respectively, resulting in relatively short predicted lifetimes.

REFERENCES

1. Susan, D.F., Marder, A.R., and Barmak, K., Thin Solid Films, 1997, 307, 133-140.

2. Susan, D.F., Ph.D. Dissertation, Lehigh University, 1999.

3. Izaki, M., Fukusumi, M., Enomoto, H., Omi, T., and Nakayama, Y., J. Japan Inst. Metals, 1993, 57 (2), 182-189.

4. Smialek, J.L. and Lowell, C.E.. J. Electrochemical Soc., 1974, 121 (6), 800-805.

5. Levine, S.R., Met. Transactions, 9A, 1978, 1237-1250.

6. Hindam, H. and Smeltzer, W.W., J. Electrochemical Soc., 1980, 127 (7), 1622-1630.

7. Shida, Y., Stott, F.H., Bastow, B.D., Whittle, D.P., and Wood G.C., Oxidation of Metals, 1982, 18 (3/4), 93-113.

8. Stott, F.H., Shida, Y., Whittle, D.P., Wood, G.C., and Bastow, B.D., Oxidation of Metals, 1982, 18 (3/4), 127-146.

9. Hindam, H. and Whittle, D.P., J. Materials Science, 1983, 18, 1389-1404.

10. Brady, M.P., Pint, B.A., Tortorelli, P.F., Wright, I.G., and Hanrahan, R.J., in Corrosion and Environmental Degradation of Materials, Vol. 19, Materials Science and Technology, eds. R.W. Cahn, P. Haasen, E. Kramer, 1999.

11. Jost, W., Diffusion in Solids, Liquids, and Gases, 1952, Academic Press Inc., New York.

12. Reed-Hill, R.E. and Abbaschian, R., Physical Metallurgy Principles, 3rd Ed., 1992, PWS-Kent Publishing, Boston, MA, 360-376.

13. Watanabe, M., Horita, Z., and Nemoto, M., Defect and Diffusion Forum, 1997, Vol. 143-147, 345-350.

14. Janssen, M.M.P., Met. Trans., 1973, 4 (6), 1623-1633.

15. Sauer, F. and Freise, V., Z. Elektrochem., 1962, 66, pg. 353.

16. Crank, J., The Mathematics of Diffusion, 2nd Ed., 1975, Clarendon Press, Oxford, 11-21.

17. Nesbitt, J.A., Vinarcik, E.J., Barrett, C.A., and Doychak, J., Mat. Sci. and Engineering A, 1992, A153, 561-566.

18. Nesbitt, J.A. and Heckel, R.W., Thin Solid Films, 1984, 119, 281-190.

19. Strutt and Vecchio, Met. Mat. Transactions, 1999, 30A, 355-362.

20. Doychak, J., in Intermetallic Compounds: Vol. 1, Principles, 1994, ed. J.H. Westbrook and R.L. Fleischer, John Wiley & Sons Ltd.

21. Whittle, D.P., Corrosion Science, 1972, 12, 869-872.

22. Jansenn, M.M.P. and Rieck, G.D., Trans. AIME, 1967, 239, 1372-1385.

23. Watanabe, M., Horita, Z., and Nemoto, M., Defect and Diffusion Forum, 1997, Vol. 143-147, 637-642.

24. Pettit, F.S., Trans. AIME, 1967, 239, 1296-1305.

25. Fink, P.J. and Heckel, R.W., in Proc. Conf. High Temperature Coatings, Orlando, FL, Oct. 1986, AIME, 21-38, 1987.

26. Perez, P., Gonzalez-Carrasco, J.L., and Adeva, P., Oxidation of Metals, 1997, 48 (1/2), 143-170.

27. Perez, P., Gonzalez-Carrasco, J.L., and Adeva, P., Oxidation of Metals, 1998, 49 (5/6), 485-507.

28. Giggins, C.S. and Pettit, F.S., J. Electrochemical Soc., 1971, 118, 1782-1790.

29. Tolpygo, V.K. and Clarke, D.R., Acta Mater., 1998, 46 (14), 5153-5166.

30. Tolpygo, V.K. and Clarke, D.R., Acta Mater., 1998, 46 (14), 5167-5174.

31. Nesbitt, J.A. and Heckel, R.W., Met. Transactions, 1987, 18A, 2061-2073.

32. Nesbitt, J.A. and Heckel, R.W., Oxidation of Metals, 1988, 29 (1/2), 75-101.

33. Nesbitt, J.A. and Lei, J-F, in Elevated Temperature Coatings: Science and Technology III, 1999, eds. J.M. Hampikian and N.B. Dahorte, TMS, 131-142.

34. ASM Handbook, Vol. 3, 10th Ed., 1992, H. Baker (ed.), American Society for Materials International, Materials Park, OH.
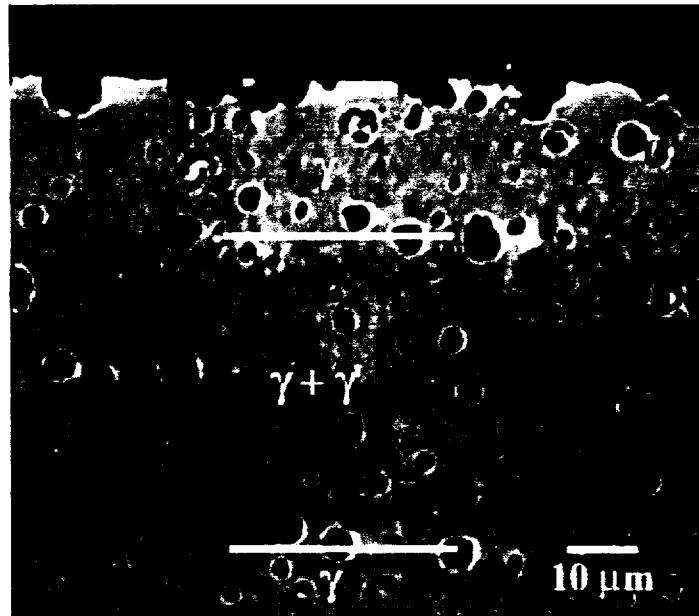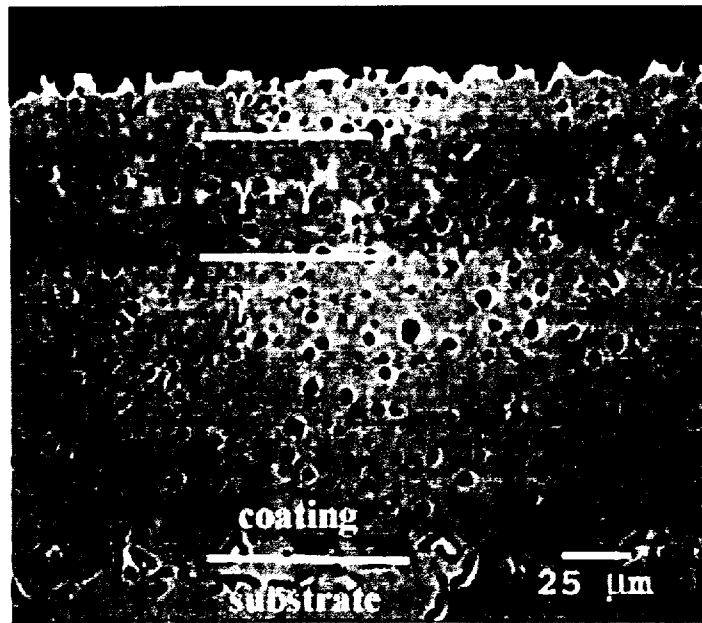
Figure 1. BSE photomicrographs of Ni-Al coating after 50 hours at 1000°C showing a) entire coating cross-section and b) close-up of γ + γ' layer and pores.
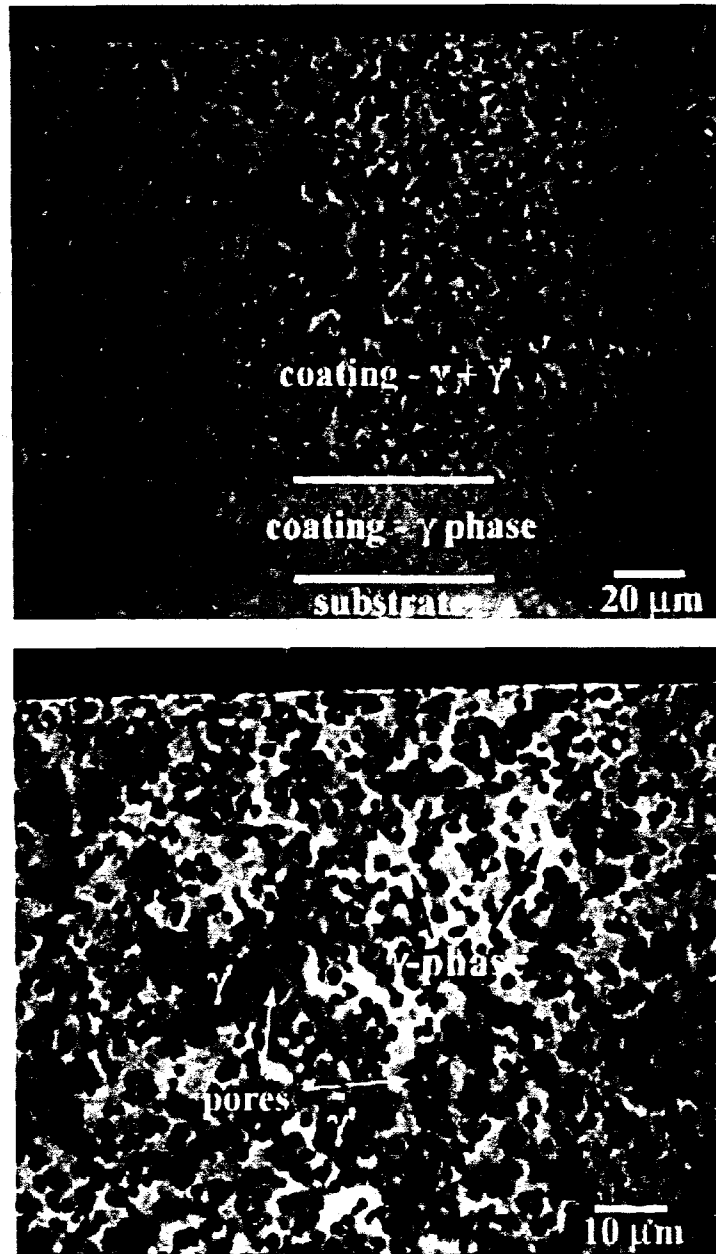
Figure 2. BSE photomicrographs of Ni-Al coating after 2000 hours at 800°C showing a) coating cross-section and b) higher magnification view of γ, γ', and pores.
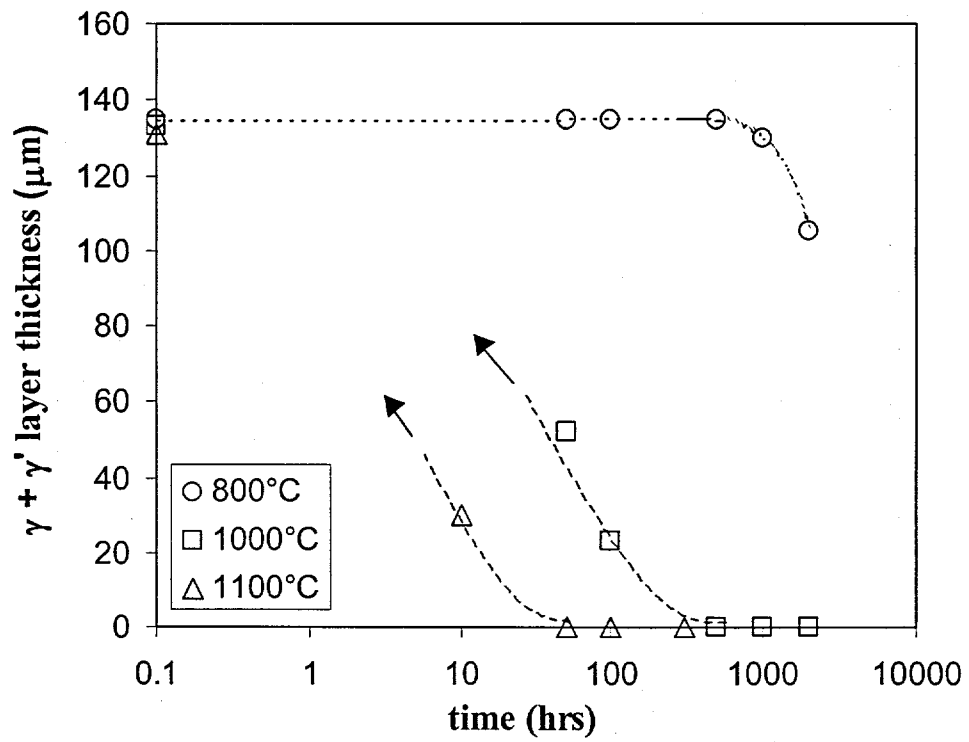
Figure 3. Thickness of γ + γ' region in Ni-Al coatings as a function of time.
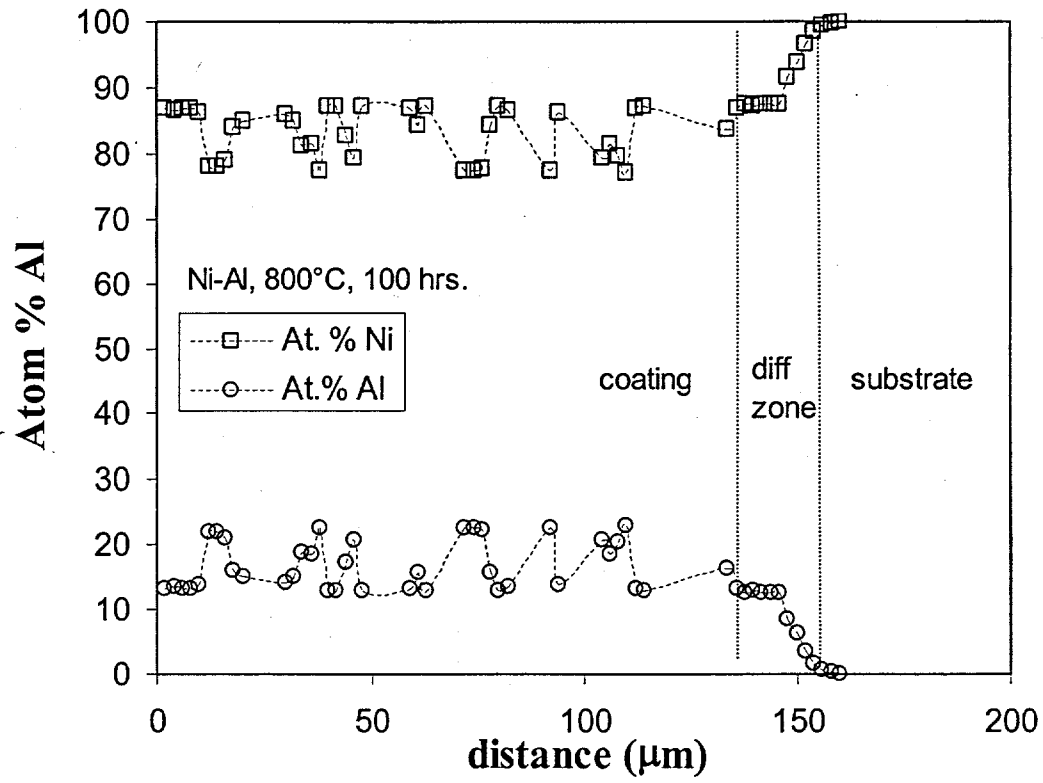
Figure 4a. EPMA profile of Ni-Al coating after 100 hours at 800°C.
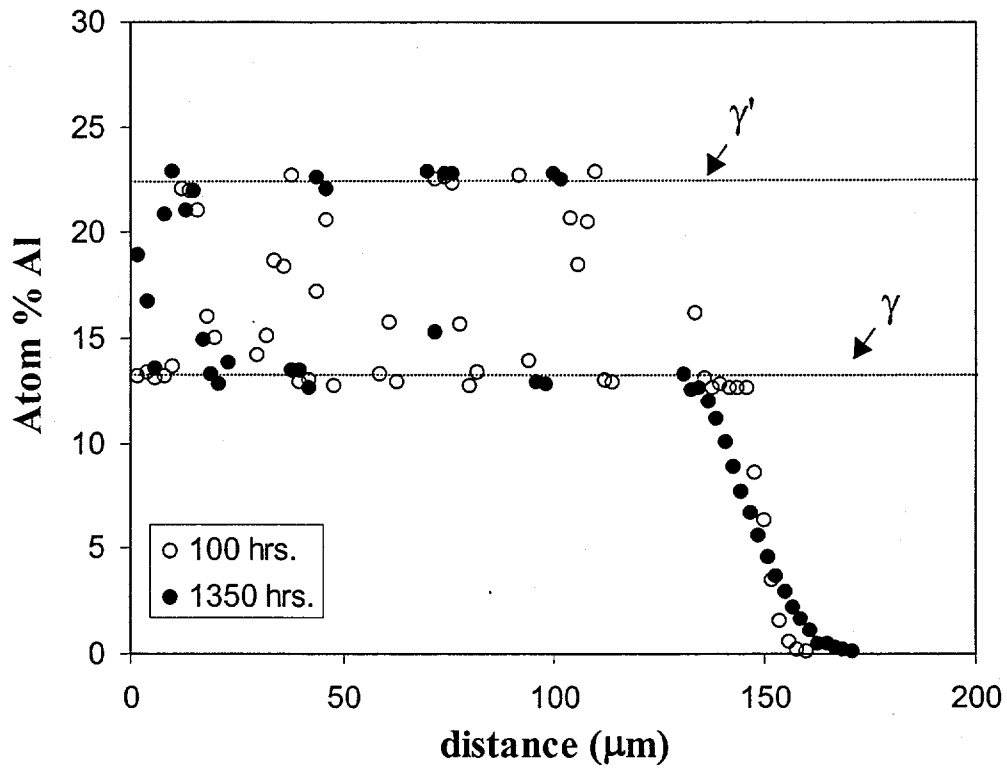
Figure 4b. Al composition profiles for 800°C samples after 100 and 1350 hours.
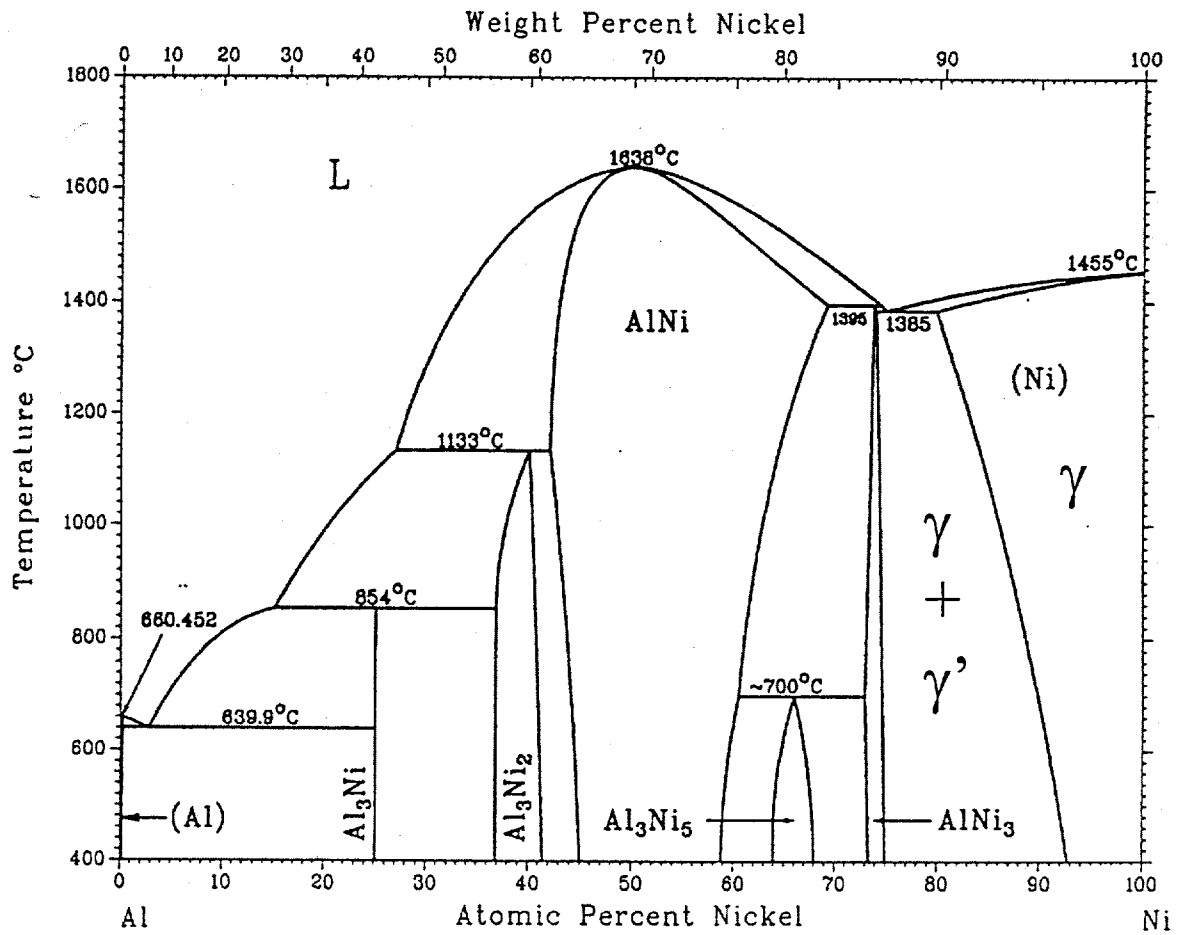
Figure 5. Ni-Al equilibrium phase diagram (adapted from Ref. [34]).
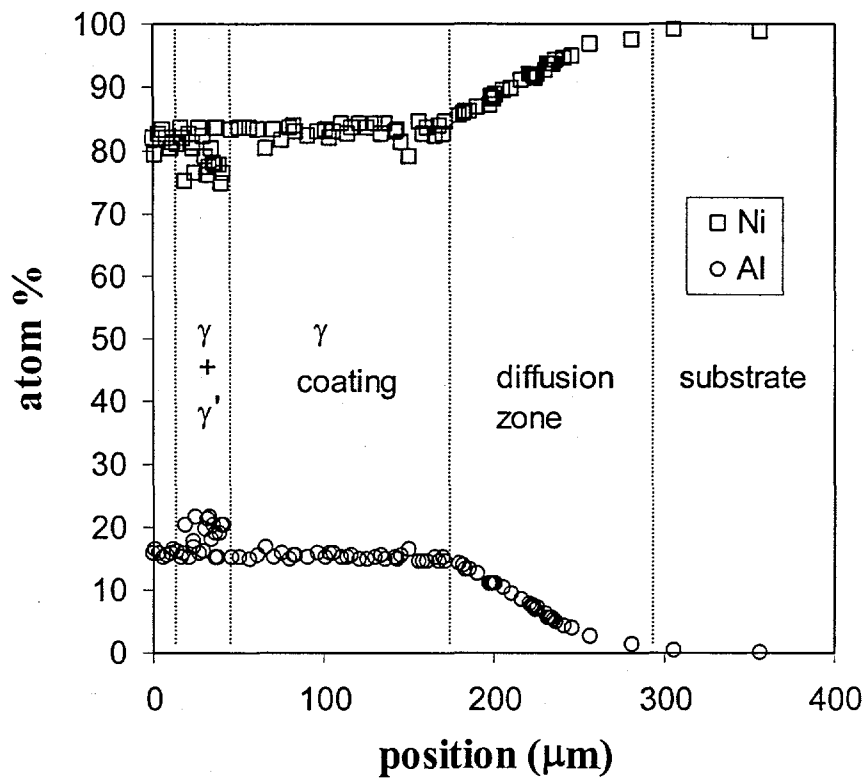
Figure 6a. EPMA profile of Ni-Al coating after 100 hours at 1000°C.
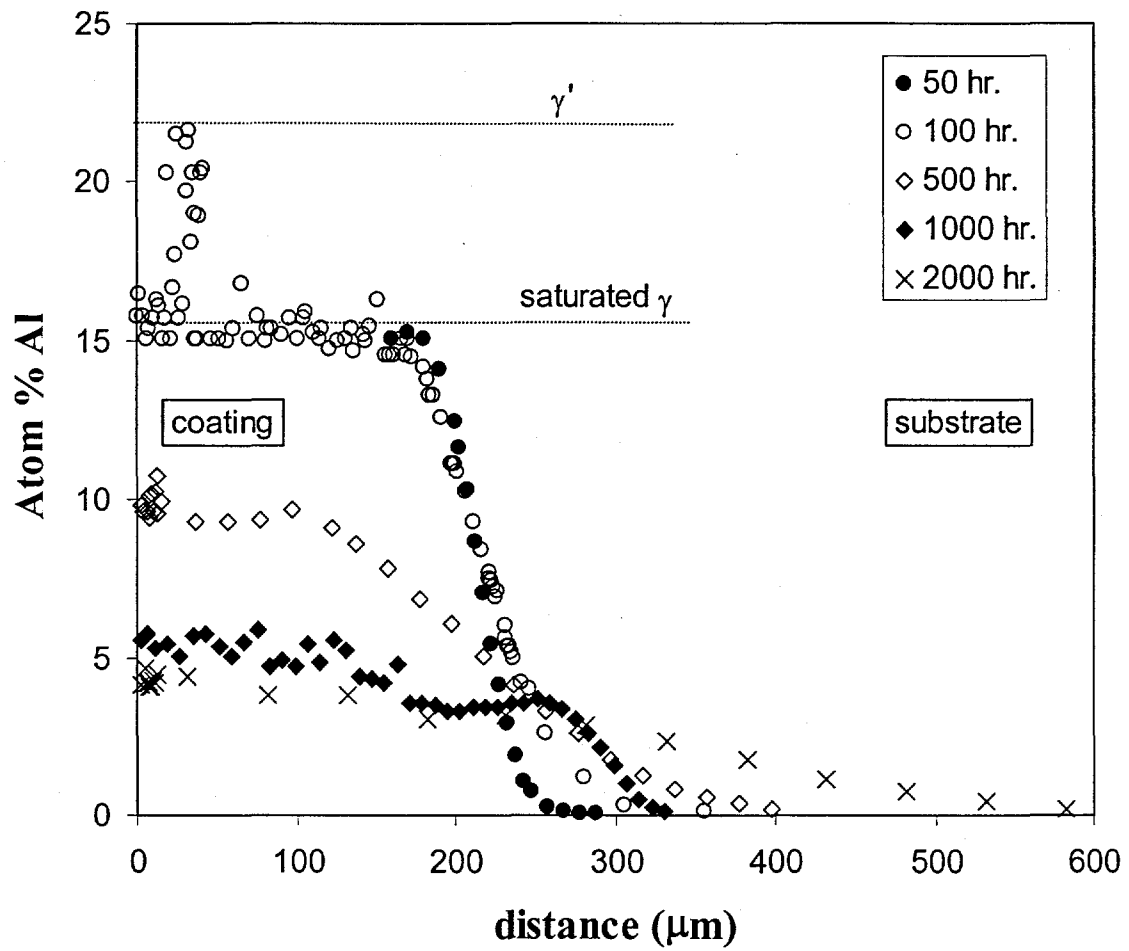
Figure 6b. Summary of Al composition profiles at 1000°C.
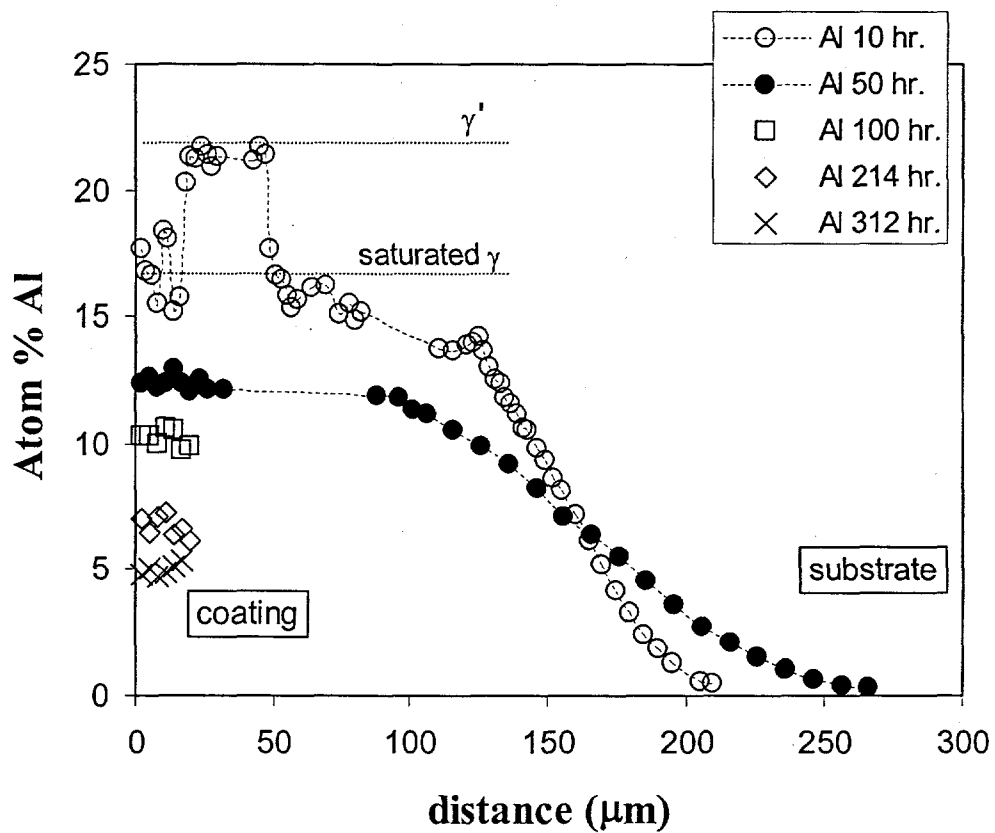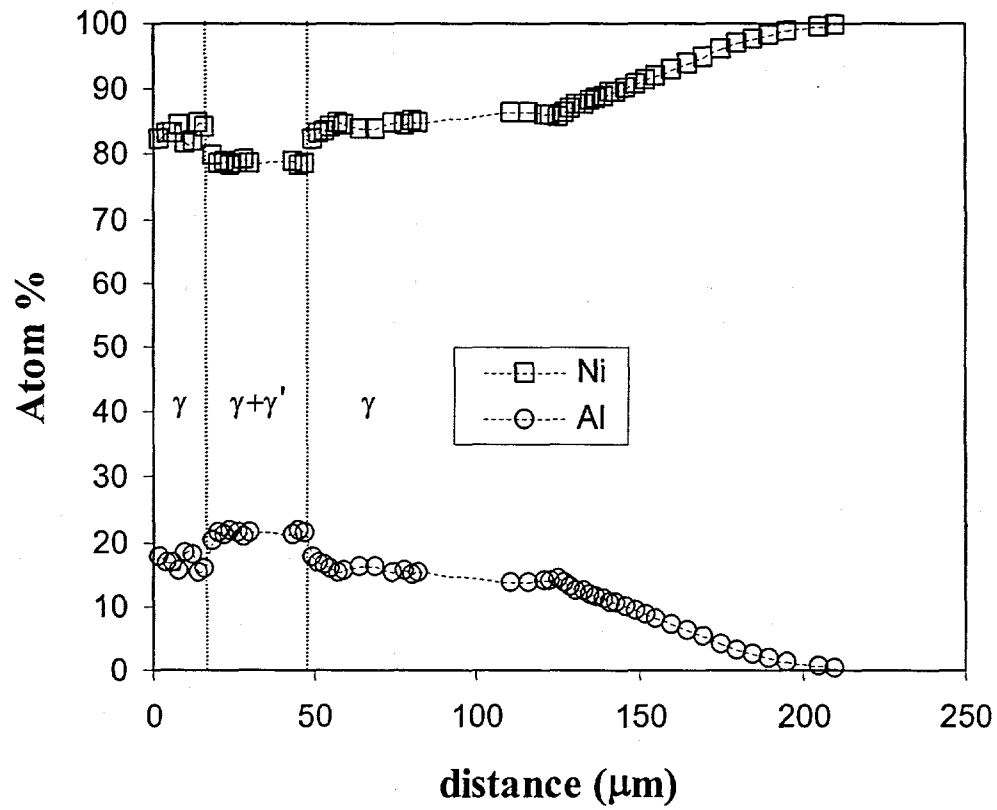
Figure 7. a) EPMA profile of 1100°C-10 hour Ni-Al coating and b) summary of Al composition profiles at 1100°C.
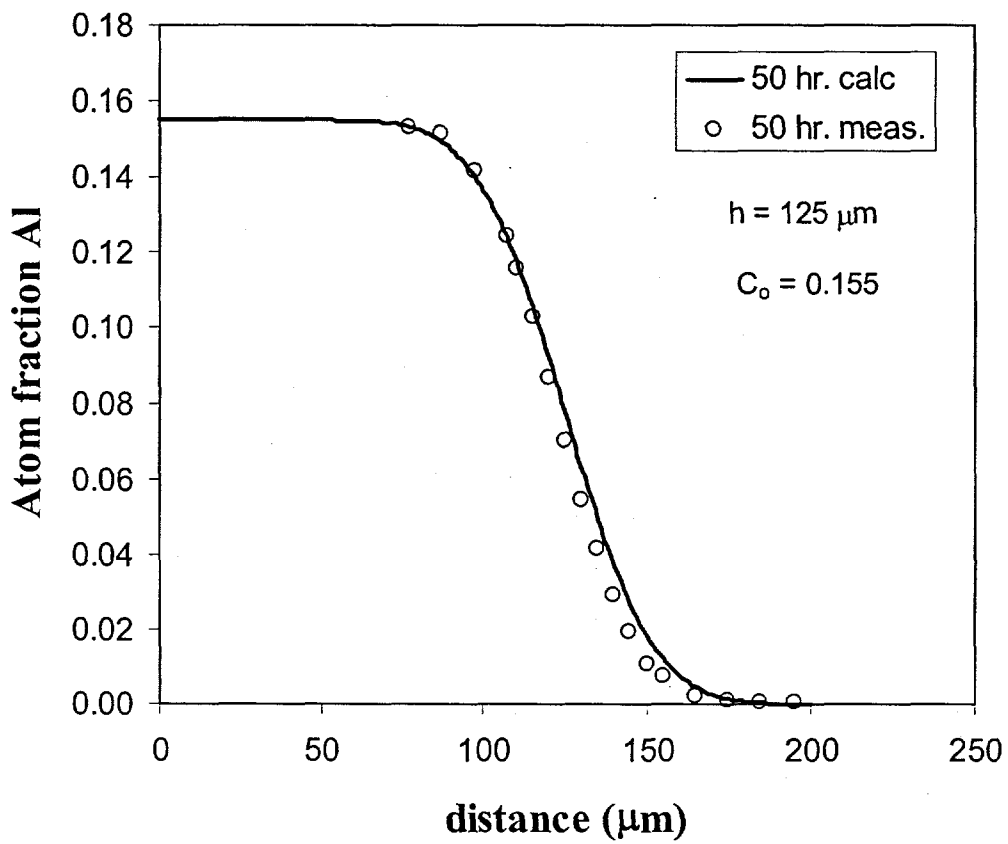
Figure 8. Measured (EPMA) and calculated diffusion profiles for 50 hours at 1000°C.
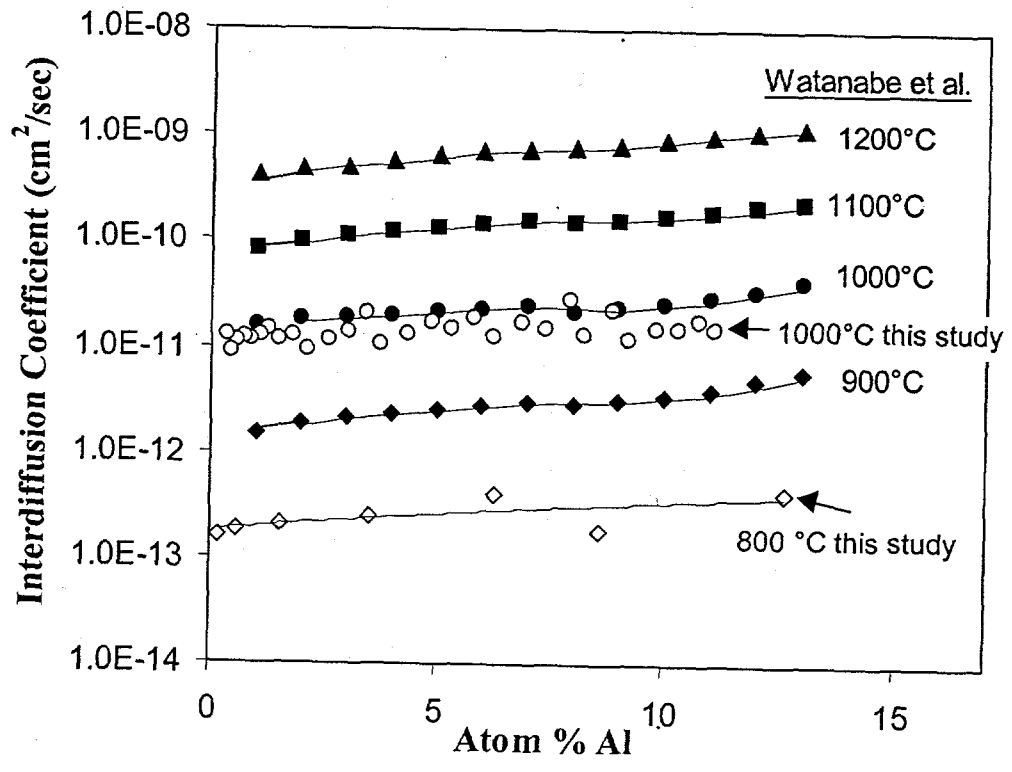
Figure 9. Interdiffusion coefficients obtained in this study at 800 and 1000°C and data from Watanabe et al. [23] for 900-1200°C.
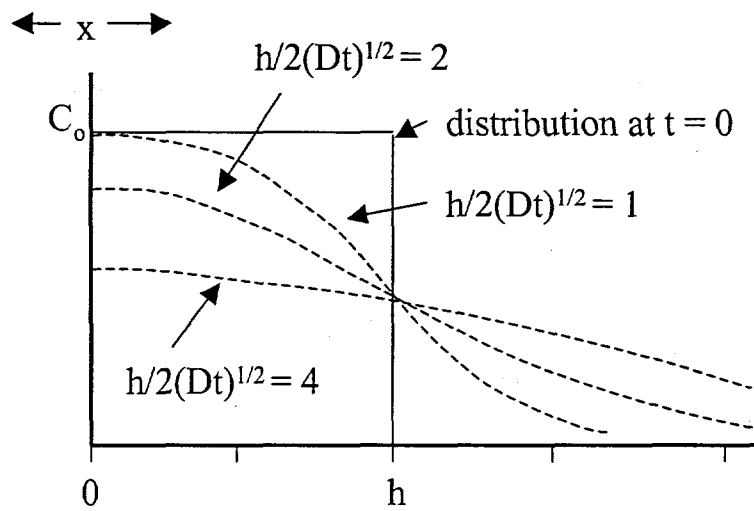
The function $C = (C_o/2)\left[erf\left(\dfrac{h+x}{2\sqrt{Dt}}\right) + erf\left(\dfrac{h-x}{2\sqrt{Dt}}\right)\right]$ for diffusion out of a plate.

Figure 10. Coating/substrate model geometry and concentration profiles according to Equation (1). (Adapted from [11])
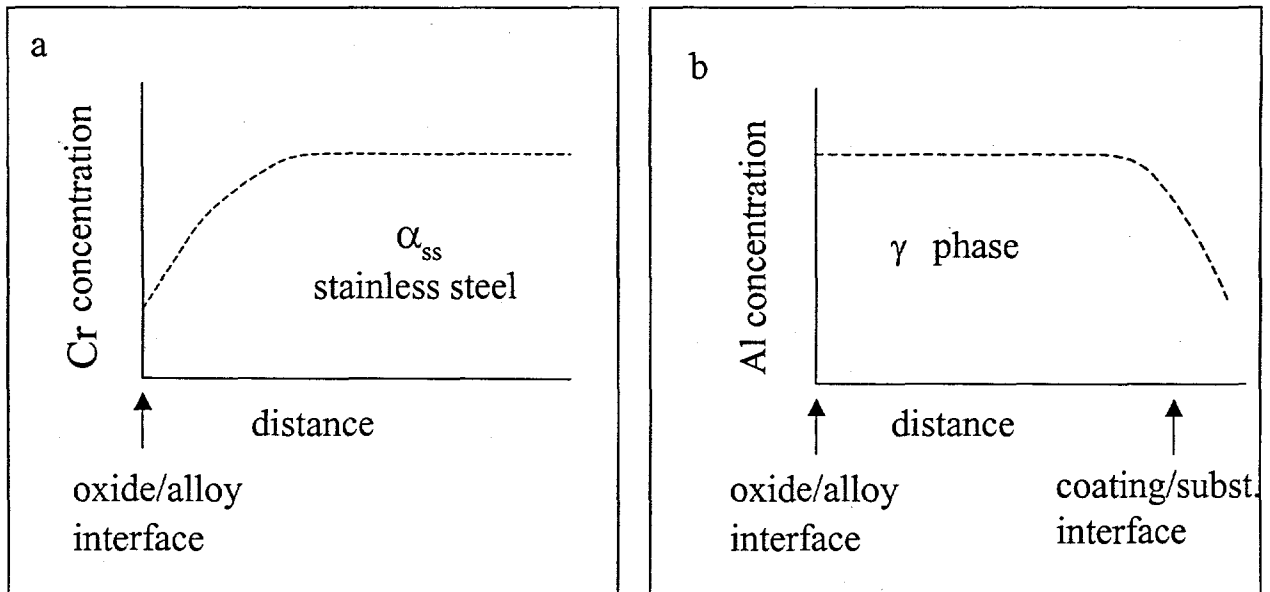
Figure 11. Schematic diagrams of a) Cr depletion below oxide in stainless steel and b) γ phase Al profile below oxide in Ni-Al coatings (after depletion of γ').
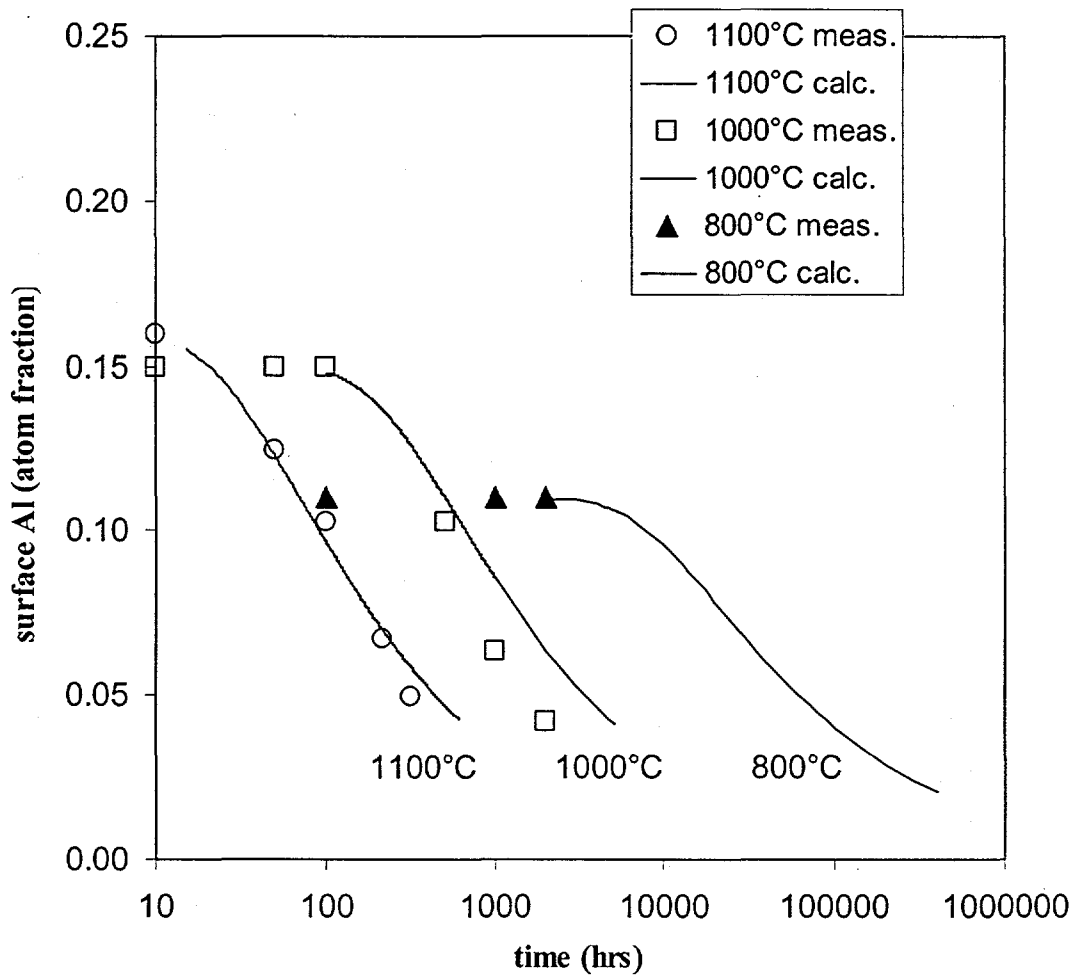
Figure 12. Measured (EPMA) and calculated surface Al concentrations as a function of time at 800, 1000, and 1100°C.
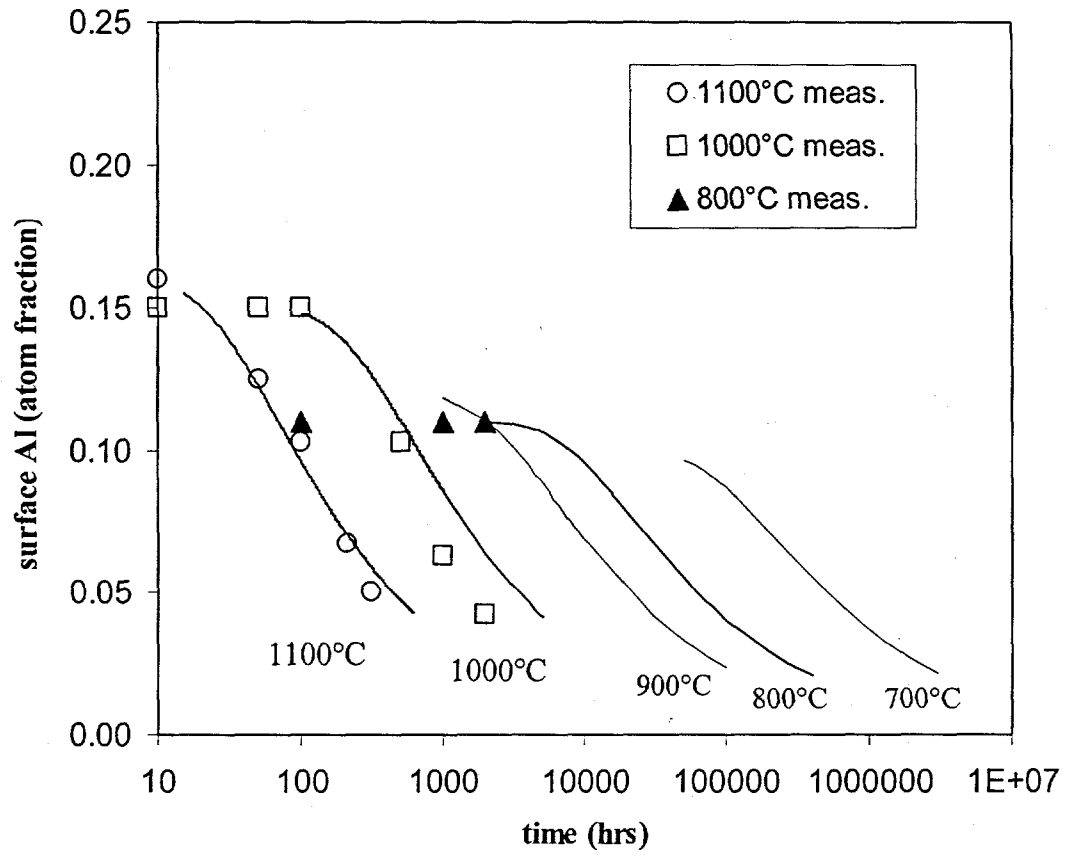
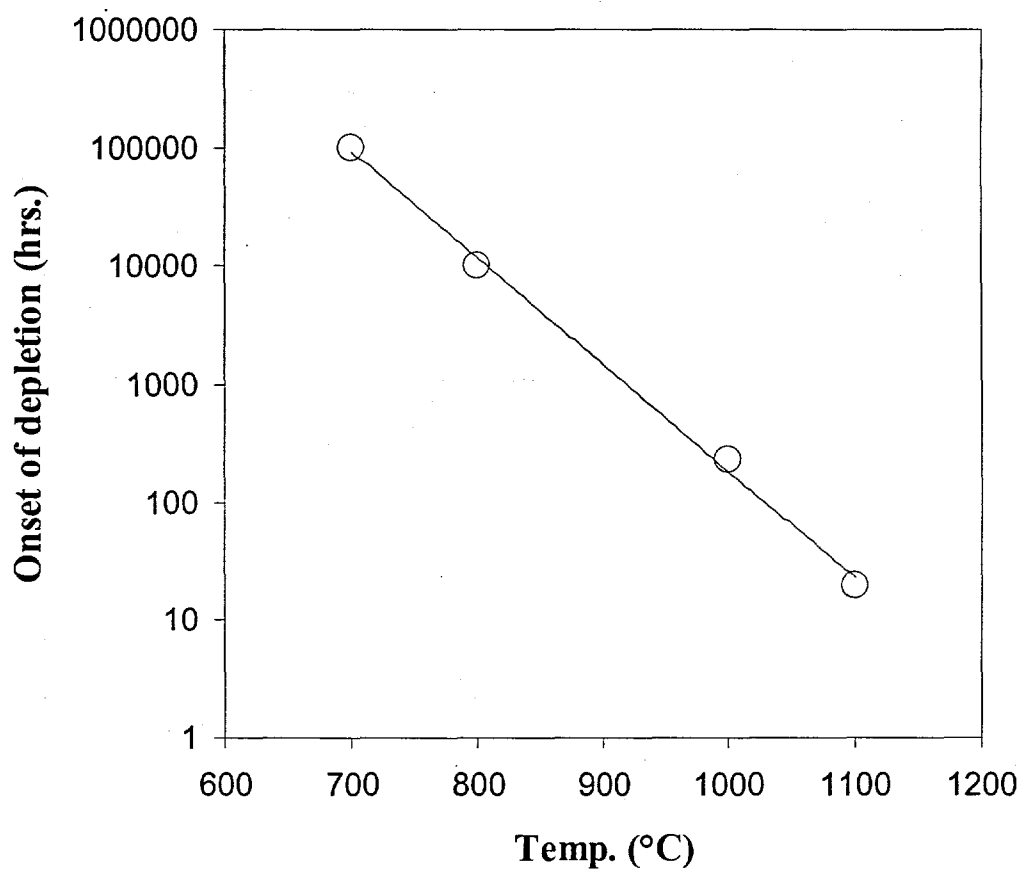Figure 13. Model results for surface Al content at 700 - 1100°C.

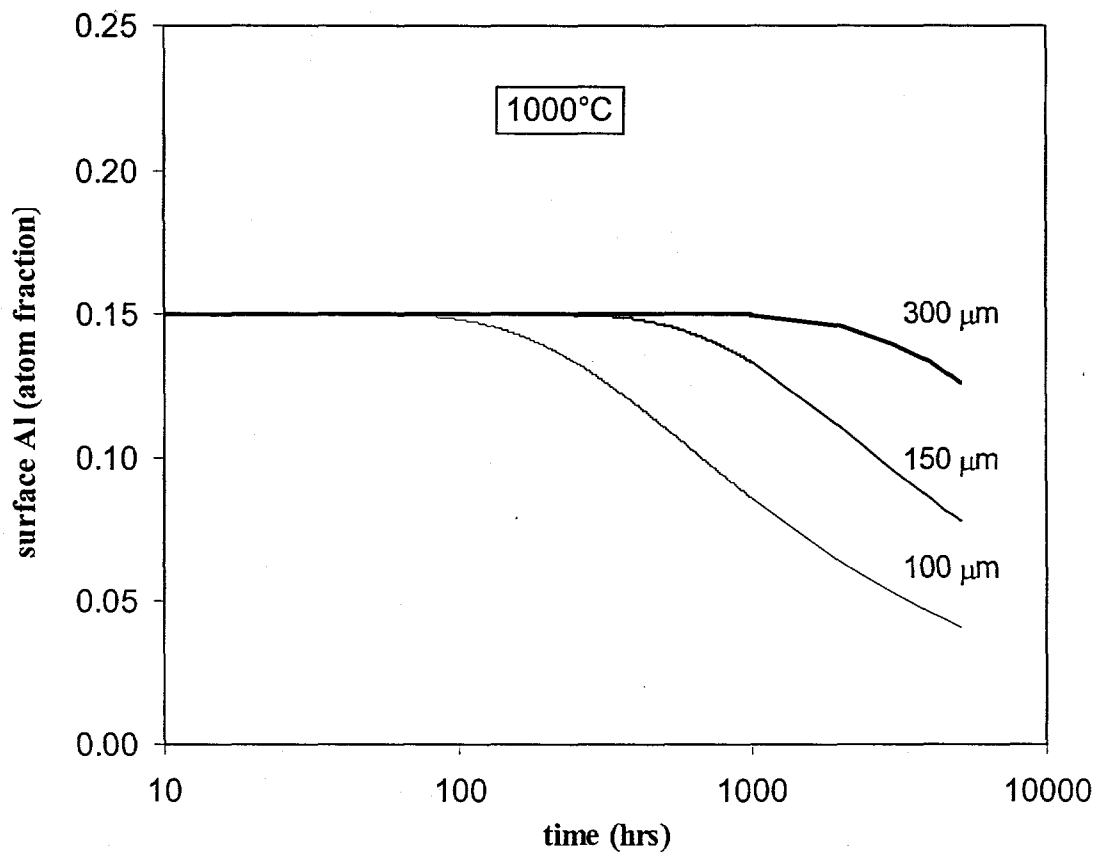Figure 14. Time to onset of depletion (1% decrease in Al) vs. temperature.

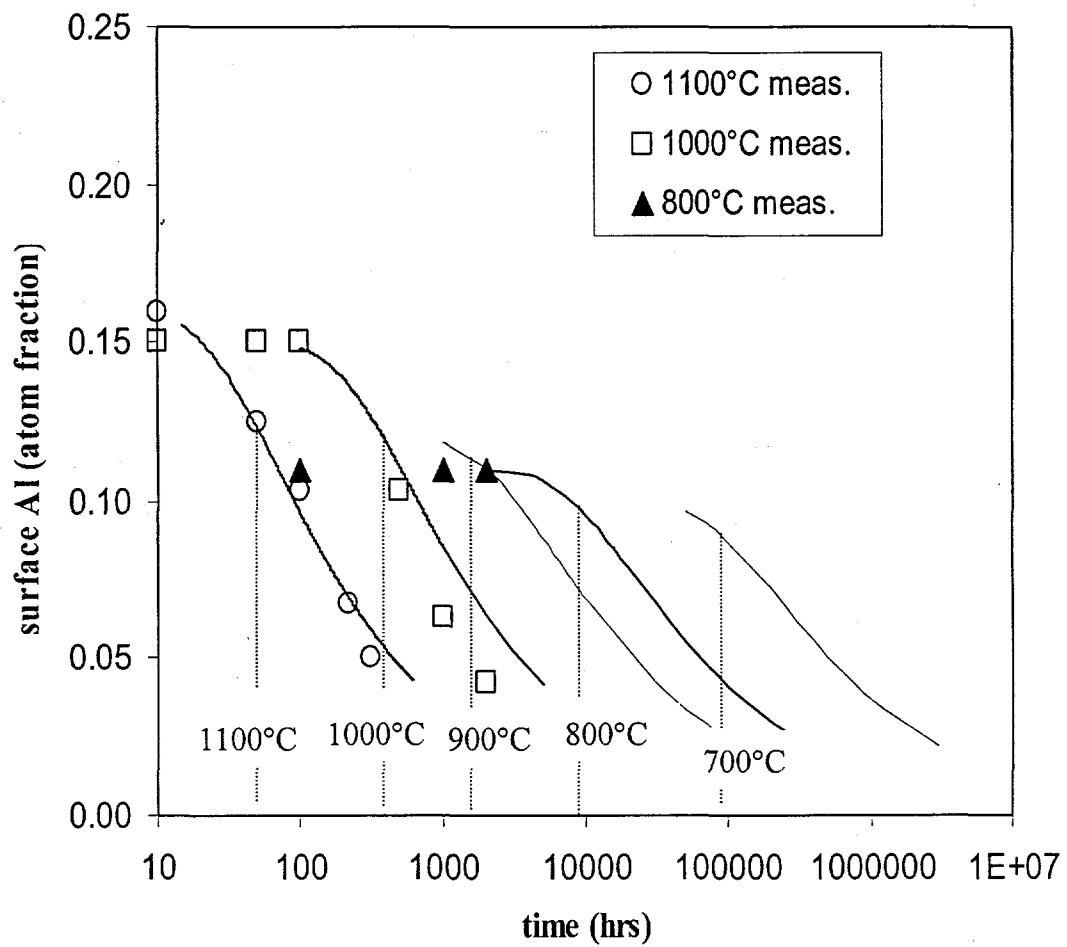Figure 15. Effect of coating thickness on surface Al content at 1000°C.

Figure 16. Model results for surface Al content with superimposed vertical lines indicating approximate coating lifetimes for 700 - 1100°C.